Chemical Science

ROYAL SOCIETY OF CHEMISTRY

EDGE ARTICLE

View Article Online
View Journal | View Issue

Cite this: *Chem. Sci.*, 2021, **12**, 1343

All publication charges for this article have been paid for by the Royal Society of Chemistry

Cerium–quinone redox couples put under scrutiny†

Uwe Bayer, Daniel Werner, Andreas Berkefeld, Cäcilia Maichle-Mössmer and Reiner Anwander *

Received 14th August 2020
Accepted 22nd November 2020

DOI: 10.1039/d0sc04489j

rsc.li/chemical-science

Homoleptic cerous complexes $Ce[N(SiMe_3)_2]_3$, $[Ce\{OSi(OtBu)_3\}_3]_2$ and $[Ce\{OSi^iPr_3\}_3]_2$ were employed as thermally robust, weakly nucleophilic precursors to assess their reactivity towards 1,4-quinones in non-aqueous solution. The strongly oxidizing quinones 2,3-dichloro-5,6-dicyano-1,4-benzoquinone (DDQ) or tetrachloro-1,4-benzoquinone (Cl_4BQ) readily form hydroquinolato-bridged ceric complexes of the composition $[(Ce^{IV}L_3)_2(\mu_2\text{-}O_2C_6R_4)]$. Less oxidising quinones like 2,5-di-*tert*-butyl-1,4-benzoquinone (tBu_2BQ) tend to engage in redox equilibria with the ceric hydroquinolato-bridged form being stable only in the solid state. Even less oxidising quinones such as tetramethyl-1,4-benzoquinone (Me_4BQ) afford cerous semiquinolates of the type $[(Ce^{III}L_2(thf)_2)(\mu_2\text{-}O_2C_6Me_4)]_2$. All complexes were characterised by X-ray diffraction, ^1H, $^{13}C\{^1H\}$ and ^{29}Si NMR spectroscopy, DRIFT spectroscopy, UV-Vis spectroscopy and CV measurements. The species putatively formed during the electrochemical reduction of $[Ce^{IV}\{N(SiMe_3)_2\}_3]_2(\mu_2\text{-}O_2C_6H_4)$ could be mimicked by chemical reduction with $Co^{II}Cp_2$ yielding $[(Ce^{III}\{N(SiMe_3)_2\}_3)_2(\mu_2\text{-}O_2C_6H_4)][Co^{III}Cp_2]_2$.

Introduction

Quinones are multifunctional organic molecules exhibiting intriguing redox behaviour.[1,2] Of particular note is their importance in biological electron–transfer processes (photosynthesis, respiration)[3] and in industrial catalysis (anthraquinone process for hydrogen peroxide production).[4] Quinones can engage in one or two electron redox processes involving the formation of either semiquinolates or hydroquinolates.[5] Strikingly, the reduction potential of 1,4-benzoquinones (*para*-benzoquinones) can easily be modified by introducing electron-withdrawing or donating substituents into the benzene ring.[5,6] As a consequence, tetrachloro-1,4-benzoquinone (chloranil, Cl_4BQ) and even more so 2,3-dichloro-5,6-dicyano-1,4-benzoquinone (DDQ) emerged as efficient oxidants in organic synthesis.[7] DDQ has been further successfully applied in photoredox catalysis.[8] Moreover, anionic η^4-1,4-benzoquinone manganese tricarbonyl features a quinoid π-complex, broadly used for the fabrication of supramolecular metal–organometallic coordination networks.[9] Relatedly, deprotonated variants of 2,5-dihydroxy-1,4-benzoquinone (DHBQ) were shown to act as rigid ditopic linkers,[10] *e.g.*, to support the formation of pentagonal dodecahedral $Ce_2(H_2O)_{18}$ cages or in permanently porous aluminium frameworks.[11] DHBQ was also probed as a bridging redox-active ligand in bimetallic $[LnCl_2(thf)_3]_2(\mu\text{-bobq})$ (Ln = Y, Dy; bobq = 2,5-bisoxide-1,4-benzoquinolato) to build single-molecule magnets.[12] More recently, the related semiquinolato radical-bridged dimeric complexes $[LnCl_2(thf)_3(\mu\text{-}Me_4sq)]_2$ (Ln = Y, Gd) were obtained by oxidation of the corresponding *in situ* formed hydroquinolate complexes with $FeCl_3$.[13] Semiquinolato-bridged scandium(III) species were reported to promote self-organised electron transfer from d-transition metals (Ir, Fe) to 1,4-quinones.[14,15]

Targeted metal-redox chemistry with quinones has been a recurring issue for the rare-earth-metal couples Ln(II)/Ln(III)[16] and Ce(III)/Ce(IV).[17] Especially in the case of molecular cerium chemistry,[17] its unique single-electron-transfer (SET) pathway has recently been extended beyond the traditional application of ceric ammonium nitrate (CAN; redox potential of 1.61 V *vs.* NHE) in organic synthesis[18] to photoredox catalysis.[19] On the other hand, redox protocols are known to provide efficient access to metalorganic Ce^{IV} complexes. Typically, such $Ce^{III} \rightarrow Ce^{IV}$ transformations are promoted by halogenating oxidants (*e.g.* C_2Cl_6, Ph_3CCl, $PhICl_2$, $TeCl_4$, $FcPF_6$, $FcBF_4$, Ph_3CBF_4, Ph_3CPF_6, I_2),[20] silver salts (AgX, X = F, I, BF_4, OTf)[21] or dioxygen.[20b,22]

Archetypical 1,4-benzoquinone (BQ) has been established as a versatile oxidant for the synthesis of homoleptic ceric complexes CeL_4 from cerous ate complexes $[CeL_4M(do)_x]$ *via* tandem oxidation-ligand redistribution protocols (L =

Institut für Anorganische Chemie, Eberhard Karls Universität Tübingen (EKUT), Auf der Morgenstelle 18, 72076 Tübingen, Germany. E-mail: reiner.anwander@uni-tuebingen.de; Web: [http://uni-tuebingen.de/syncat-anwander]

† Electronic supplementary information (ESI) available. CCDC 2022461, 2022462, 2022463, 2022464, 2022465, 2022466, 2022467, 2022468, 2022469, 2022470, 2022471, 2022472, 2022473, 2022474, 2022475 and 2022476. For ESI and crystallographic data in CIF or other electronic format see DOI: 10.1039/d0sc04489j

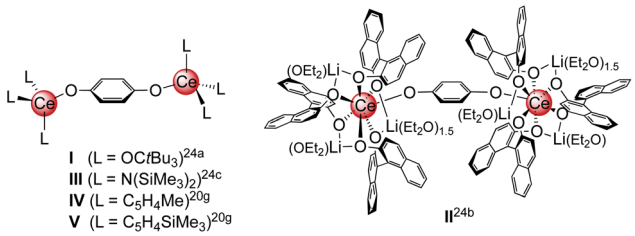

Chart 1 Structurally characterised dicerium(IV) hydroquinolate complexes (**I–V**),[20g,24] obtained *via* oxidation of cerous precursor with BQ.

monoanionic ligand, M = alkali metal and do = donor solvent; separation of an alkali-metal hydro-/semiquinolate).[23] In the presence of sterically demanding ligands L, BQ was also shown to form hydroquinolato (hq)–bridged ceric complexes of the general composition $[L_3Ce–OC_6H_4O–CeL_3]$.[20g,24] This very $Ce^{III} \rightarrow Ce^{IV}$ transformation was pioneered by Sen *et al.* in 1992, resulting in the isolation of $[(tBu_3CO)_3Ce(OC_6H_4O)Ce(OCtBu_3)_3]$ (Chart 1, **I**).[24a] In the same paper, the oxidation of $Ce(OCtBu_3)_3$ with 2,6-di-*tert*-butyl-1,4-benzoquinone to the terminal Ce^{IV}-semiquinolate radical $(tBu_3CO)_3Ce(O_2C_6H_2tBu_2)$ was described as evidenced by ^1H NMR and EPR spectroscopic measurements.[24a] More recently, Schelter *et al.* reported on hq-bridged complex **II** resulting from the oxidation of cerous $Ce(BINOlate)_3(thf)Li_3(thf)_4$ with 0.5 equivalents of BQ.[24b] Similarly, our group synthesized $[Ce\{N(SiMe_3)_2\}_3]_2(\mu_2\text{-}O_2C_6H_4)$[24c] (**III**) and $(CeCp^R_3)_2(\mu_2\text{-}O_2C_6H_4)$ ($Cp^R = C_5H_4Me$ (**IV**) and $C_5H_4(SiMe_3)$ (**V**)).[20g] In contrast, the reaction of BQ with $[Ce(Me_2pz)_3]_x$ featuring the sterically less demanding and increasingly nucleophilic 3,5-dimethylpyrazolato ligand (Me_2pz) led in fact to a transient Ce^{IV} hydroquinolate species (as indicated by the characteristic colour change), which, however, at ambient temperature was converted into the isolable trimetallic Ce^{III} complex $Ce_3(pchd)_2(Me_2pz)_5(thf)_2$ (pchd = 1,4-bis(3,5-dimethylpyrazol-1-yl)cyclohex-2,5-diene-1,4-diolato).[23c] Apparently, the new pchd ligand formed *via* 1,4-nucleophilic attack at bq by two adjacent Me_2pz ligands. This nucleophilic reaction pathway could be prevented by using bulky *t*Bu groups on the pz ligand, but homolpetic $Ce(tBu_2pz)_4$ was formed as the main ceric product *via* irreversible ligand rearrangement.[23c]

As such, cerium–1,4-benzoquinone couples have revealed distinct redox chemistry, we became curious about as to what extent such redox transformations are affected by both the type of 1,4-benzoquinone oxidant and the molecular Ce^{III} precursor. The present study uncovers some unexpected correlation between Ce^{IV}–hydroquinolato stabilisation and quinone oxidant strength, as well as a new path to *p*-semiquinolato–radical-bridged rare-earth-metal complexes.

Results and discussion

Molecular redox precursors

The quinones used in this study comprise 2,3-dichloro-5,6-dicyano-1,4-benzoquinone (DDQ), tetrachloro-1,4-benzoquinone (Cl_4BQ), 1,4-benzoquinone (BQ), tetramethyl-1,4-benzoquinone (Me_4BQ), 2,5-di-*tert*-butyl-1,4-benzoquinone (tBu_2BQ), 1,4-naphthoquinone (NQ), and 9,10-anthraquinone (AQ). All are commercially available and were selected according to their reduction potentials spanning a E^0 range of 89 to 887 mV ($2e^-/2H^+$, *vs.* NHE, *cf.*, Scheme 1).[5,25] The cerous precursors were chosen according to the criteria solubility, weak nucleophilicity, proven access to the tetravalent state, and a stabilizing effect on the latter. Furthermore, the use of sterically bulky ligands was assumed to minimise the occurrence of ligand redistribution reactions. Accordingly, homoleptic Ce $[N(SiMe_3)_2]_3$ (**1**) appeared to be an ideal benchmark system.[24c] After additional investigations into the respective pyrazolate

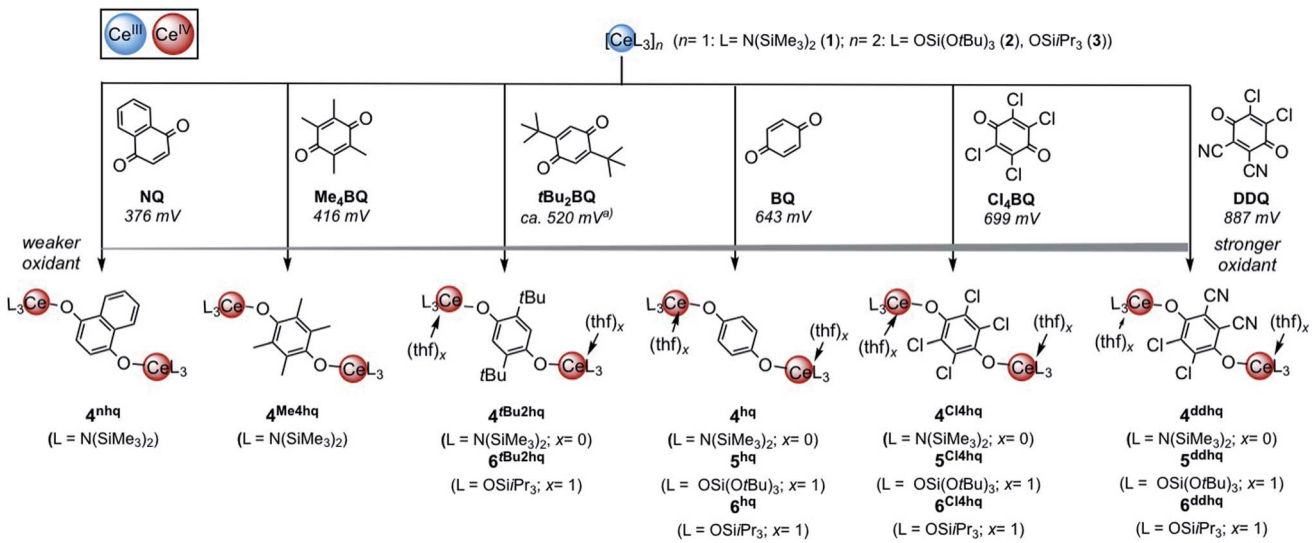

Scheme 1 Oxidation of trivalent cerium complexes with 1,4-quinone derivatives under formation of hydroquinolato-bridged ceric complexes. To enable better assessment of the relative oxidation ability $2e^-/2H^+$ reductions potentials are given in mV *versus* NHE according to ref. 5. (*a*) Calculated value.

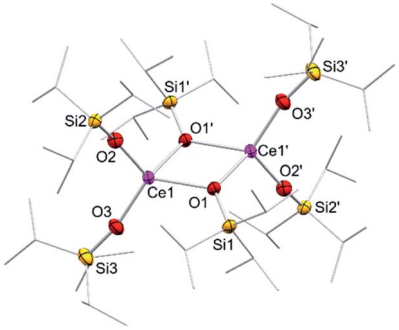

Fig. 1 Crystal structure of $[Ce\{OSi^iPr_3\}_3]_2$ (**3**). Ellipsoids are shown at the 50% probability level. Hydrogen atoms are omitted for clarity. Selected interatomic distances [Å] and angles [°]: Ce1–O1 2.3951(12), Ce1–O2 2.1659(14), Ce1–O3 2.1671(14); Ce1–O2–Si2 163.03(9), Ce1–O3–Si3 167.40(10).

chemistry, the abovementioned $[Ce(R_2pz)_3]$ (R = Me, *t*Bu) were discarded because of persisting alternative reaction pathways like 1,4-nucleophilic attack of BQ by Me_2pz and ligand redistribution (formation of $Ce(tBu_2pz)_4$).[23c] The new pyrazolate studies clearly confirmed that steric hindrance of both the pyrazolato ligand and the 1,4-benzoquinone can minimise/counteract such undesired reactions, but the formation of product mixtures seems inevitable. Products crystallised from these reactions include minor amounts of ceric $[Ce(tBu_2pz)_3(thf)]_2(Me_4hq)$ or a cerous product of partial pyrazolyl-promoted nucleophilic attack $Ce_3(bpad)(pasq)(Me_2pz)_6(thf)$ (bpad = 1,4-bis(3,5-dimethylpyrazol-1-yl)anthra-1,4-diolato; pasq = 1-(3,5-dimethylpyrazol-1-yl)anthra-1,4-semiquinolato) (84%) mixed with semiquinolate $[Ce(Me_2pz)_2(thf)_2(asq)]_2$ (asq = anthra-semiquinolato; *cf.* ESI† for structural details). The use of Ce^{III} halides was discarded mainly for solubility issues.

In addition to silylamide **1**, the siloxide derivatives $[Ce\{OSi(OtBu)_3\}_3]_2$ (**2**)[21d,26] and $[Ce(OSi^iPr_3)_3]_2$ (**3**) were assessed as suitable cerous precursors. Complexes **2** and **3**, with and without intramolecular donor site, respectively, were readily obtained in pure form *via* protonolysis of **1** with the corresponding silanol.[26] The crystal structure of the new complex **3** revealed a dimeric arrangement with two μ_2-bridging and four terminal siloxy groups (Fig. 1), similar to that found for tris(*tert*-butoxy)siloxy congener **2** or $[Ce(OSiPh_3)_3]_2$ [27] or $[Ce(OCHtBu_2)_3]_2$.[28] The Ce–$O_{terminal}$ (2.1659(14) and 2.1671(14) Å) and the Ce–O_{μ_2} distances (2.3951(12) and 2.4030(12) Å) of **3** are slightly shorter than those in **2** (Ce–$O_{terminal}$ 2.202(3), 2.186(3) Å; Ce–$O_{\mu2}$ 2.532(2) Å) and $[Ce(OSiPh_3)_3]_2$ (Ce–$O_{terminal}$ 2.141(7), 2.185(6) Å; Ce–$O_{\mu2}$ 2.345(6), 2.583(5) Å) reflecting the lower coordination number (CN 4 *vs.* 5), but slightly longer than in $[Ce(OCHtBu_2)_3]_2$ (Ce–$O_{terminal}$ 2.142(2), 2.152(3) Å; Ce–$O_{\mu2}$ 2.363(3) Å).[28] The ^{1}H NMR spectrum of **3** in C_6D_6 shows two singlets at −28.82 and −17.23 ppm for the μ_2-OSi^{i}Pr$_3$ groups and two singlets at 6.46 and 9.09 ppm for the terminal siloxy ligands indicating a non-fluxional dimeric species in non-coordinating solvents. When recorded in THF-d_8, only two signals for the OSi^{i}Pr$_3$ groups appeared, in accordance with the formation of a monomeric adduct $[Ce\{OSi^iPr_3\}_3(thf\text{-}d_8)_x]$.

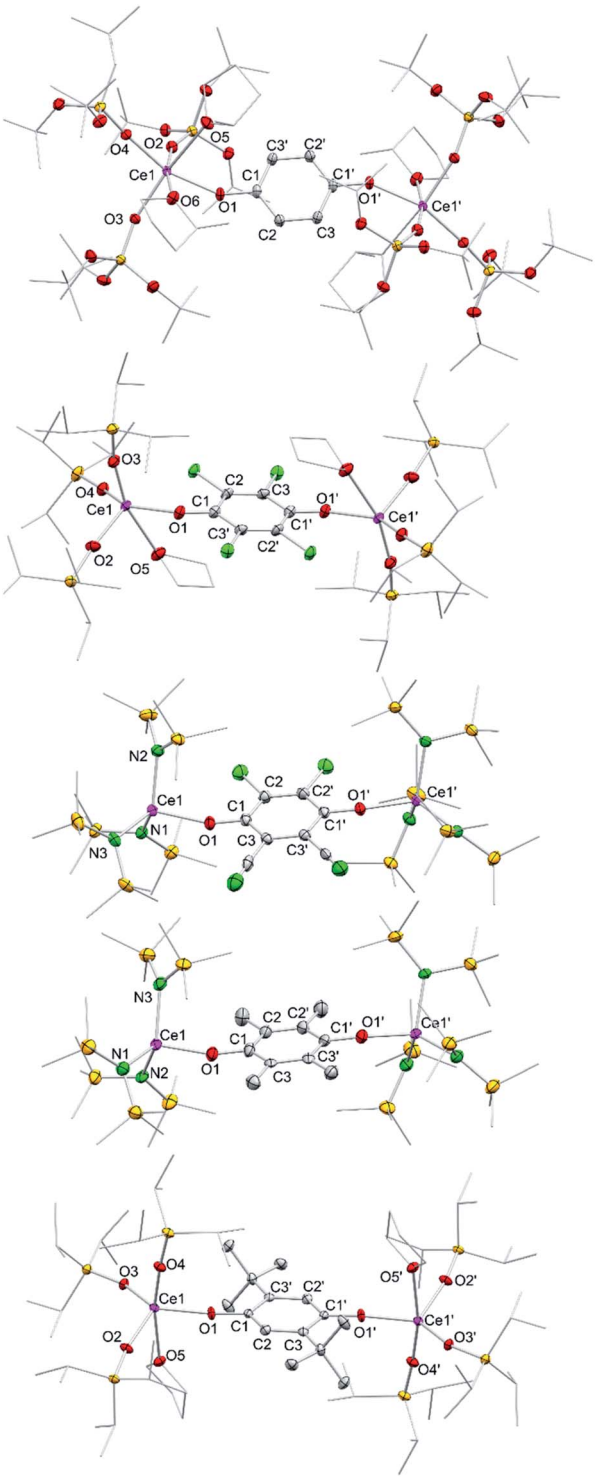

Fig. 2 Crystal structures of $[Ce\{OSi(OtBu)_3\}_3(Me\text{-}thf)_{2|2}(\mu_2\text{-}O_2C_6H_4)$ (5^{hq}·2MeTHF), $[Ce\{OSi^iPr_3\}_3(thf)]_2(\mu_2\text{-}O_2C_6Cl_4)$ (6^{Cl4hq}), $[Ce\{N(SiMe_3)_2\}_3]_2(\mu_2\text{-}O_2C_6Cl_2CN_2)$ (4^{ddq}), $[Ce\{N(SiMe_3)_2\}_3]_2(\mu_2\text{-}O_2C_6Me_4)$ (4^{Me4hq}), and $[Ce\{OSiiPr_3\}_3(thf)]_2(\mu_2\text{-}O_2C_6tBu_2H_2)$ (6^{tBu2hq}) (from top down). Ellipsoids are shown at the 50% probability level. Hydrogen atoms, disordered ligands and lattice solvents are omitted for clarity. Selected interatomic distances for 5^{hq}, 6^{Cl4hq}, 4^{ddq}, and 4^{Me4hq} are given in Tables 1 and 2. Selected bond lengths for 6^{tBu2hq} [Å]: Ce1–O1 2.109(3), Ce1–O2 2.104(3), Ce1–O3 2.097(3), Ce1–O4 2.107(3), C1–C2 1.391(6), C2–C3 1.391(6), C1–C3′ 1.405(6), C1–O1 1.350(5).

Table 1 Selected analytical data of complexes 4^{hq}, 4^{Cl4hq}, 4^{ddhq}, 4^{Me4hq}, 4^{tBu2hq}, 4^{nhq}. Interatomic distances are given in [Å], angles in [°], chemical shifts in [ppm], μ_{eff} in [BM], UV/Vis absorption band in [nm], and E_{pc}/E_{pa} in [V *vs.* Fc/Fc$^+$]

Complex	4^{hq}[24c]	4^{Cl4hq}	4^{ddhq}	4^{Me4hq}	4^{tBu2hq}	4^{nhq}
Ce1–O1	2.0895(13)	2.149(4)	2.1731(15)	2.082(6)	2.117(2)	—
Ce1–N1	2.2388(14)	2.265(5)	2.2206(18)	2.280(7)	2.235(2)	—
Ce1–N2	2.2398(15)	2.230(5)	2.2112(18)	2.229(7)	2.246(2)	—
Ce1–N3	2.2487(14)	2.244(5)	2.2467(19)	2.238(7)	2.259(2)	—
C–C$_{arom}$	1.387(3)–1.399(2)	1.383(8)–1.392(8)	1.390(4)–1.407(3)	1.390(11)–1.408(12)	1.388(4)–1.405(4)	—
C1–O1	1.356(2)	1.324(7)	1.318(3)	1.366(10)	1.378(3)	—
Ce1–O1–C1	173.13(11)	156.1(4)	161.02(15)	162.4(6)	146.79(18)	—
^{1}H NMR[a]	0.43	0.45	0.45	0.43[d]	0.49	0.44
^{13}C{^{1}H} NMR[a]	—	—	5.6	—	—	5.6
^{29}Si{^{1}H} NMR[a]	—	−8.1	−7.3	−8.8	—	−8.1
μ_{eff}	0.67	0.68	0.59	0.89	—	1.19
UV-Vis absorption bands[b]	485	319/518	384/511	362/411/681	—	339/425/474/677
E_{pc}[c]	−0.699/−0.966	−0.415/−0.624	−0.546	—	—	—
E_{pa}[c]	−0.558	−0.290	−0.1685	—	—	—
$E_{1/2}$	−0.76	−0.46	−0.36			
ΔE	0.408	0.334	0.377	—	—	—

[a] NMR spectra recorded in C_6D_6. [b] UV-Vis spectra recorded in toluene. [c] Determined in THF using c(analyte) = 2 mM and c(electrolyte) = 0.1 M and a scan rate of 50 mV s^{-1}. [d] Determined in toluene-d_8 at 0 °C.

Quinone oxidation of Ce[N(SiMe$_3$)$_2$]$_3$ (1)

Treatment of Ce[N(SiMe$_3$)$_2$]$_3$ (**1**) with each 0.5 equivalents of DDQ, Cl$_4$BQ, Me$_4$BQ, *t*Bu$_2$BQ and NQ, in a mixture of toluene and *n*-hexane, immediately led to a colour change from yellow to dark brown. Upon recrystallisation from toluene/*n*-hexane mixtures it was possible to isolate the hydroquinolato-bridged complexes [Ce{N(SiMe$_3$)$_2$}$_3$]$_2$(μ$_2$-O$_2$C$_6$Cl$_4$) (**4^{Cl4hq}**), [Ce{N(SiMe$_3$)$_2$}$_3$]$_2$(μ$_2$-O$_2$C$_6$Cl$_2$(CN)$_2$) (**4^{ddhq}**), [Ce{N(SiMe$_3$)$_2$}$_3$]$_2$(μ$_2$-O$_2$C$_6$Me$_4$) (**4^{Me4hq}**), [Ce{N(SiMe$_3$)$_2$}$_3$]$_2$(μ$_2$-O$_2$C$_6$*t*Bu$_2$H$_2$) (**4^{tBu2hq}**) and [Ce{N(SiMe$_3$)$_2$}$_3$]$_2$(μ$_2$-O$_2$C$_{10}$H$_6$) (**4^{nhq}**) in very good crystalline yields of 71 to 90% (Scheme 1). The crystal structures of the new complexes **4^{xhq}** are isostructural to the previously reported derivative **4^{hq}**[24c] and only differ in the bridging hq linker (Fig. 2). The Ce1–O1 distances of 2.084(6) to 2.173(2) Å (for a full list of interatomic distances see Table 1) are in the same range as found for other hq-bridged cerium complexes (2.086(10)–2.143(5) Å).[20g,24] Likewise, the Ce1–N bond lengths compare well to other Ce^{IV} silylamides like [Ce{N(SiMe$_3$)$_2$}$_3$]$_2$(μ$_2$-O$_2$C$_6$H$_4$) (2.2388(14)–2.2487(14) Å),[24c] Ce[N(SiMe$_3$)$_2$]$_3$Cl (2.217(3) Å),[20a] and Ce[N(SiHMe$_2$)$_2$]$_4$ (2.2378(11)–2.2574(11) Å).[20d] Also, the C–C distances of the hq linker converge as the expected aromatic ring is formed and the C–O distances of 1.318(3) to 1.378(3) Å corroborate the formation of C–O single bonds.

The ^{1}H NMR spectra of compounds **4^{xhq}** in C_6D_6 show singlets for the trimethylsilyl (TMS) groups at 0.43 to 0.45 ppm along with signals for the bridging hydroquinolato moieties.

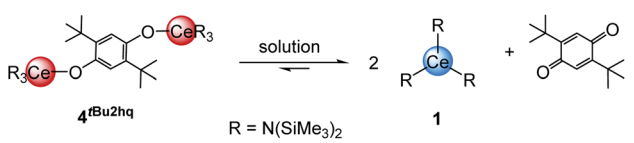

Scheme 2 Equilibrium between **4^{tBu2hq}** and reformation of reactants in solution and solid state.

Further, the ^{13}C{^{1}H} NMR spectra of **4^{ddhq}** and **4^{nq}** display a singlet for the TMS groups at 5.6 ppm and signals in the aromatic region for the different hydroquinolates, indicative of a successful reduction of the respective benzoquinone derivatives. The characterisation of **4^{tBu2hq}** in solution (C_6D_6) was not feasible, due to the prevailing equilibrium shown in Scheme 2, and ready back-formation of **1** and 2,5-di-*tert*-butyl-1,4-benzoquinone.

While the ^{1}H NMR spectrum of **4^{tBu2hq}** primarily shows signals for the starting materials and only minor product signals, its DRIFT spectrum indicated the absence of any strong C=O absorption band, and therefore the stability of **4^{tBu2hq}** in the solid state (see Fig. S10 and S45 in ESI†). In contrast, complexes **4^{hq}**, **4^{Cl4hq}** and **4^{ddhq}** derived from the stronger oxidizing quinones are very stable in the solid state and in solution. This fits again well with the already pronounced instability of **4^{Me4hq}** and **4^{nhq}** which slowly decompose in *n*-hexane and toluene at ambient temperature and rapidly undergo decomposition in THF. Tracking of the progress of the decomposition by ^{1}H NMR spectroscopy revealed the formation of **1** and other paramagnetic Ce^{III} species which, however, could not be identified. The progressing decomposition can also be seen in the ligand-to-metal charge transfers observed in the UV-Vis spectra (Fig. S68, ESI†). As the spectra of **4^{hq}**, **4^{Cl4hq}** and **4^{ddhq}** show mainly one strong absorption band at around 500 nm (ε > 5060 L mol^{-1} cm^{-1}), the spectra of **4^{Me4hq}** and **4^{nhq}** show several absorption bands with significantly lower intensities (ε < 4400 L mol^{-1} cm^{-1}) indicative of Ce^{III} species and therefore redox decomposition of the compounds.

All attempts to isolate putative **4^{ahq}**, derived from the weakest oxidising quinone under study, namely 9,10-anthraquinone (E^0 = 89 mV; 2e$^-$/2H$^+$, *vs.* NHE),[5] were unsuccessful with the reaction mixtures showing no colour change immediately after addition of the anthraquinone. However, a colour change from

Table 2 Selected analytical data of complexes 5^{hq}, 5^{Cl4hq}, 5^{ddq}, 6^{hq}, 6^{Cl4hq}, 6^{ddq}. Interatomic distances are given in [Å], angles in [°], chemical shifts in [ppm], μ_{eff} in [BM], UV/Vis absorption band in [nm], and E_{pc}/E_{pa} in [V *vs.* Fc/Fc$^+$]

Complex	5^{hq}	5^{Cl4hq}	5^{ddq}	6^{hq}	6^{Cl4hq}	6^{ddq}
Ce1–O1	2.1244(10)	2.184(3)	—	—	2.207(2)	2.2325(16)
Ce1–O2	2.1534(10)	2.091(3)	—	—	2.095(2)	2.0841(16)
Ce1–O3	2.1334(11)	2.094(3)	—	—	2.066(2)	2.0710(17)
Ce1–O4	2.1396(11)	2.104(3)	—	—	2.080(2)	2.091(2)
C–C$_{arom}$	1.390(2)–1.395(2)	1.373(8)–1.406(5)	—	—	1.380(4)–1.407(4)	1.379(5)–1.415(3)
C1–O1	1.3540(17)	1.326(4)	—	—	1.322(3)	1.316(3)
Ce1–O1–C1	151.76(10)	140.0(2)	—	—	138.54(18)	144.85(14)
^{1}H NMR[a]	1.36	1.36	1.36		1.12/1.05	1.12/1.05
^{13}C{^{1}H} NMR[a]	72.5/32.6	72.8/32.4	73.0/32.5		18.0/14.0	19.1/15.1
^{29}Si{^{1}H} NMR[a]	−103.2	−104.6	−105.3	7.0	9.6	10.7
μ_{eff}	0.82	0.54	0.60	0.68	0.50	0.66
UV-Vis absorption band[b]	369/622	493	384/450	526[c]	511	381/470
E_{pc}[d]	−1.7855	−1.414	−1.353	−1.116/−1.816	−1.580	−1.149/−1.484
E_{pa}[d]	−0.3625	−0.521	0.130	−1.273/−0.817	−0.729	−0.751
ΔE	1.416	0.893	1.483	0.999	0.851	0.733

[a] NMR spectra recorded in THF-d_8. [b] Spectra recorded in toluene. [c] Spectra recorded in THF. [d] Determined in THF using c(analyte) = 2 mM and c(electrolyte) = 0.1 M and a scan rate of 50 mV s^{-1}.

yellow to green occurred after two days and the respective ^{1}H NMR spectrum showed multiple paramagnetic signals.

Quinone oxidation of siloxides [Ce{OSi(O*t*Bu)$_3$}$_3$]$_2$ (2) and [Ce{OSi^{i}Pr$_3$}$_3$]$_2$ (3)

Reacting cerous siloxides **2** and **3** with the selected quinones in THF immediately gave a colour change of the reaction mixtures (from colourless to: dark purple (BQ), dark red (Cl_4BQ), dark yellow/orange (DDQ), pale purple (tBu$_2$BQ), pale blue (Me_4BQ), pale green (NQ)). The ceric compounds [CeL$_3$(thf)]$_2$(μ_2-O$_2$C$_6$H$_4$) (5^{hq}, 6^{hq}), [CeL$_3$(thf)]$_2$(μ_2-O$_2$C$_6$Cl$_4$) (5^{Cl4hq}, 6^{Cl4hq}), [CeL$_3$(thf)]$_2$(μ_2-O$_2$C$_6$Cl$_2$(CN)$_2$) (5^{ddq}, 6^{ddq}), with L = OSi(O*t*Bu)$_3$ or OSi^{i}Pr$_3$ derived from quinones with a relatively strong oxidising effect were successfully isolated from these reactions (Scheme 1).

However, the weakly oxidizing quinones Me_4BQ and NQ did not lead to tetravalent cerium species, as indicated by the detection of only paramagnetic signals in the ^{1}H NMR spectra (for an example of such a ^{1}H NMR spectrum, see Fig. S34 in the ESI;† formation of semiquinolates, *vide infra*). The accessible complexes **5** and **6** were obtained in moderate to good crystalline yields of 42 to 71% upon recrystallisation from THF or THF/Et_2O mixtures. Crystals suitable for XRD analysis were obtained for complexes 5^{hq}, 5^{Cl4hq}, 6^{Cl4hq}, 6^{ddhq} and 6^{tBu2hq}, revealing the same structural motif as complexes **4**, that is two CeL$_3$ moieties connected *via* a hydroquinolato linker (Fig. 2).

Strikingly, the ^{1}H NMR spectrum of 6^{tBu2hq} indicated the existence of an equilibrium similar to that of ceric 4^{tBu2hq} (*cf.* Scheme 2). However, along with the reactants **3** and tBu$_2$BQ additional signals assignable to distinct dia- and paramagnetic decomposition products were detected. Further, the crystal structures of complexes **5** and **6** show that the cerium atoms are additionally coordinated by THF donor molecules. The Ce1–O$_{siloxide}$ distances of 2.066(2) to 2.1534(10) (see Table 2 for a complete list of interatomic distances) compare well to other ceric siloxides like Ce{OSi(O*t*Bu)$_3$}$_4$ (2.089(2)–2.157(2) Å [26] and 2.084–2.160 Å [21d]) or Ce{OSiPh$_3$}$_4$(dme) (2.098(1)–2.133(1) Å).[29] Also, as seen for the silylamides **4**, the Ce1–O$_{hq}$ distances of 2.1244(10) to 2.2325(16), as well as the C–C and C–O distances underline the formation of an aromatic hq linker.[20g,24] ^{1}H NMR spectroscopic measurements also validate the formation of Ce^{IV} species, showing a sharp singlet for the *tert*-butyl groups and a doublet plus a septet for the iso-propyl groups depending on the siloxy co-ligand.

Electrochemical investigation of complexes 4^{xhq}, 5^{xhq} and 6^{xhq}

Cyclic voltammetry (CV) measurements of complexes 4^{xhq}, 5^{xhq} and 6^{xhq} have been conducted at ambient temperature in 0.2 mM solutions in THF and 0.1 M [nPr$_4$N][B(C$_6$H$_3$(CF$_3$)$_2$-3,5)$_4$] as a support electrolyte, and referenced *vs.* Fc/Fc$^+$. Due to the low stability of compounds 4^{Me4hq}, 4^{tBu2hq} and 4^{nhq} in polar solvents CV measurements of these complexes were not feasible. Most of the CV measurements revealed successive quasireversible (**4**) or irreversible (**5**/**6**) Ce^{IV} → Ce^{III} reduction steps, but badly resolved (for E_{pc} values see Tables 1 and 2). The detection of two closely adjacent redox events (E_{pc} values) in some cyclic voltammograms may correspond to a successive reduction/oxidation of the cerium centres. Similar features were also described for the hq-bridged Ce(IV)–BINOLate complex **II**.[24b] All complexes under study display redox processes with a large separation of E_{pc} and E_{pa} ($\Delta E \approx$ 0.6 V for **4**; 1.5 V for **5** and 1.0 V for **6**).

Representatively, the cyclic voltammograms of the DDQ-functionalized Ce^{III}/Ce^{IV} redox couples are depicted in Fig. 3 (top graphic). The silylamide complexes **4** gave reduction potentials similar to those reported for halogenido-functionalised ceric complexes Ce[N(SiMe$_3$)$_2$]$_3$X ($E_{1/2}$ = −0.56 (X = F), −0.30 (X = Cl), −0.31 (X = Br)) with $E_{1/2}$ values of −0.46 V for 4^{Cl4hq} and −0.36 V for 4^{ddhq}.[30] Only 4^{hq} with $E_{1/2}$ = −0.76 V gave a significantly higher stabilisation by 0.20 V. The extra-large separation of the reduction/oxidation events

observed for the siloxide complexes **5** and **6** had been noticed previously for rare-earth-metal siloxides and was assigned to oxidation-state-dependent ligand reorganisation processes.[31]

Stabilisation of the tetravalent oxidation state of cerium in complexes **4**, **5**, and **6** increases in the order of $N(SiMe_3)_2$ < $OSi(OtBu_3)_3$ < OSi^iPr_3 as co-ligand (Fig. 3/bottom) which is in accordance with previous findings.[20f,26,30,31c] Surprisingly, the stabilisation of Ce^{IV} proceeds in reverse order of the oxidation potential of the 1,4-quinones under study giving the most stable complexes for the hydroquinolato-bridged complexes and the least stable compounds for its 2,3-dichloro-5,6-dicyano-hydroquinolato congeners. A reason for this trend could be the increasingly electron-deficient nature of the aromatic hydroquinolato linkers due to the large −I effect of the substituents. The Ce^{IV} oxidation state can be stabilised by increasing donor strength of the ligands.[32] Based on this, it seems surprising that isolable complexes $\mathbf{4}^{\mathbf{Me4hq}}$ and $\mathbf{4}^{\mathbf{nhq}}$, derived from weakly oxidizing quinones, are not stable in solution at ambient temperature. This might be a result of another reaction pathway preferred after formation of the hydroquinolato-bridged Ce^{IV} complexes (like following up redox processes and the formation of Ce^{III} semiquinolates, *cf.* vide infra).

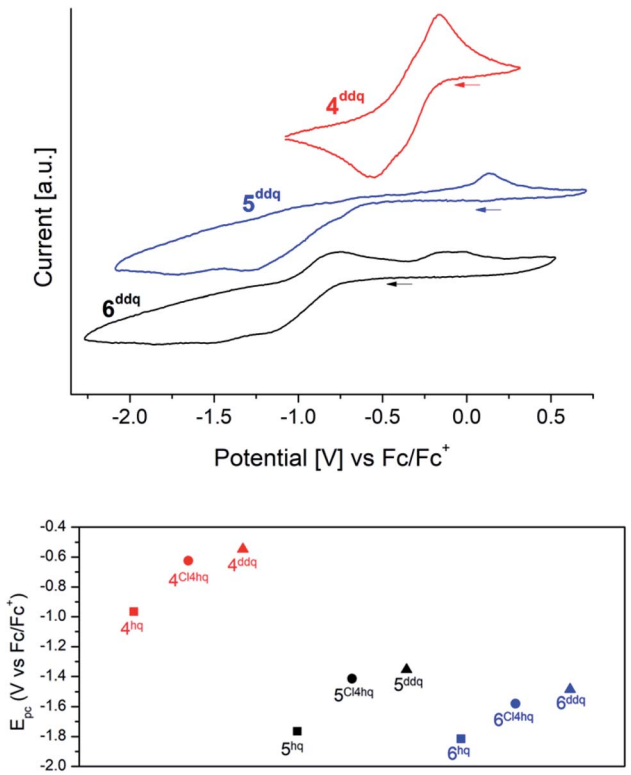

Fig. 3 Top: Stacked cyclic voltammograms of complexes $\mathbf{4}^{\mathbf{ddq}}$ (red), $\mathbf{5}^{\mathbf{ddq}}$ (blue), $\mathbf{6}^{\mathbf{ddq}}$ (black) in THF (v = 50 mV s^{-1}; c(analyte) = 2 mM; c([nPr$_4$N][B(C$_6$H$_3$(CF$_3$)$_2$-3,5)$_4$]) = 0.1 M). Bottom: comparison of the second reduction potentials of complexes **4** (red), **5** (black), and **6** (blue) in THF *vs.* Fc/Fc$^+$. Squares: complexes with bridging 1,4-hydroquinolates; cycles: complexes with bridging tetrachloro-1,4-hydroquinolates; triangles: complexes with bridging 2,3-dichloro-5,6-dicyano-1,4-hydroquinolates.

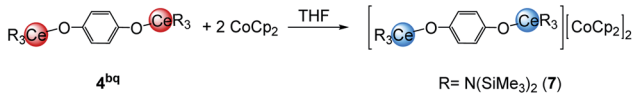

Scheme 3 Reduction of $\mathbf{4}^{\mathbf{bq}}$ with two equivalents of $CoCp_2$.

Reduction of silylamide $\mathbf{4}^{\mathbf{hq}}$ with cobaltocene

Having investigated the electrochemical reduction of compounds **4**, **5** and **6**, the chemical reduction with cobaltocene ($CoCp_2$) (−1.31 V *vs.* Fc/Fc$^+$ in DME)[2a] was attempted, as it has already been shown to engage in such reductions.[31a,33] Accordingly, treatment of a solution of $\mathbf{4}^{\mathbf{hq}}$ in THF with two equivalents of $CoCp_2$ resulted in a colour change from dark brown to pale yellow (Scheme 3). The ^{1}H NMR spectrum of the reaction mixture showed complete consumption of $CoCp_2$ and only broadened signals indicating the formation of a paramagnetic Ce^{III} species. Crystallisation from a concentrated THF-d_8 solution at −40 °C gave light brown crystals of the composition [(Ce{N(SiMe$_3$)$_2$}$_3$)$_2$(μ_2-O$_2$C$_6$H$_4$)][CoCp$_2$]$_2$ (**7**) (Fig. 4).

Complex **7** shows the same structural motif as $\mathbf{4}^{\mathbf{hq}}$ but is flanked by two cobaltocenium cations. Compared to $\mathbf{4}^{\mathbf{hq}}$, the Ce–N and Ce1–O1 distances are elongated by approximately 0.19 Å as expected for the larger Ce^{III} ion size.[34] On the contrary, the bonding parameters within the bridging hydroquinolato linker did not change, further corroborating a cerium-borne redox chemistry. Reacting $\mathbf{4}^{\mathbf{hq}}$ with one equivalent of $CoCp_2$ did not lead to a mixed $Ce^{III/IV}$ complex but gave a mixture of 50% of **7** and 50% of unreacted starting material.

The reactions of $CoCp_2$ with other complexes **4** to **6** in THF-d_8 showed immediate decolourisation of the solution while the ^{1}H NMR spectra of the reaction mixtures displayed only paramagnetic signals (for an example, see Fig. S33 in the ESI†). However, the isolation of additional reduced species similar to **7** was not successful.

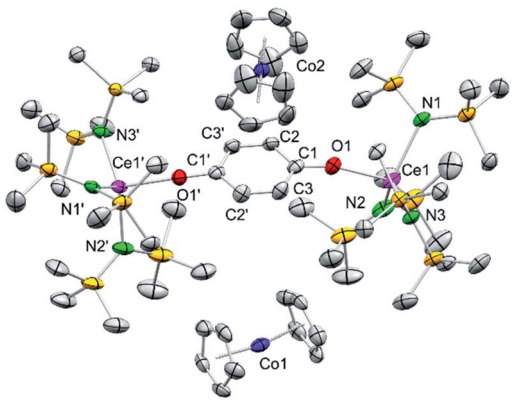

Fig. 4 Crystal structure of [(Ce{N(SiMe$_3$)$_2$}$_3$)$_2$(μ_2-O$_2$C$_6$H$_4$)][CoCp$_2$]$_2$ (**7**). Ellipsoids are shown at the 50% probability level. Hydrogen atoms, disordering of the cyclopentadienyl ligands and lattice THF are omitted for clarity. Selected interatomic distances [Å]: Ce1–N1 2.420(2), Ce1–N2 2.402(2), Ce1–N3 2.418(2), Ce1–O1 2.202(2), C1–O1 1.344(4), C1–C2 1.391(4), C1–C3 1.392(4), C2–C3′ 1.392(4).

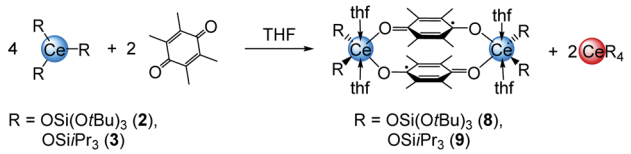

Scheme 4 Formation of cerous semiquinolates **8** and **9** from the reaction of **2** or **3** with Me_4BQ.

Cerium semiquinolates

A closer look at the reactions of cerous siloxides **2** and **3** with the weakly oxidising quinone Me_4BQ (which did not produce any tetravalent cerium species; *vide supra*) revealed another important detail of the cerium–quinone redox system. Treatment of **2** or **3** with 0.5 equivalents of Me_4BQ led to a colour change from colourless to light blue. Upon recrystallisation from THF dark blue crystals suitable for X-ray diffraction could be grown and were identified as cerous semiquinolates $[CeL_2(thf)_2]_2(\mu_2\text{-}O_2C_6Me_4)_2$ (with L = $OSi(OtBu)_3$ (**8**) or OSi^iPr_3 (**9**)) (Scheme 4).

Examining the reaction mixtures by ^1H NMR spectroscopy in THF-d_8 showed, besides paramagnetic signals for **8** and **9**, a sharp singlet at 1.39 ppm (for **8**) or a doublet plus a septet at 1.13 and 1.04 ppm (for **9**), indicating the formation of homoleptic $Ce[OSi(OtBu)_3]_4$ or $[Ce(OSi^iPr_3)_4]$, respectively, as a result of the one-electron reduction of Me_4bq followed by ligand redistribution. Crucially, such a reaction pathway seems unfeasible for complexes **4**, since putative homoleptic "$Ce[N(SiMe_3)_2]_4$" is unknown.[20a] Emergent kinetic constraints in the case of ceric complexes **4** were also suggested by the redox behaviour of $[Ce\{N(SiHMe_2)_2\}_3]_2$ derived from a less bulky silylamido ligand. Accordingly, the cerous bis(dimethylsilyl)amide complex was treated with one equivalent of both BQ and Me_4BQ in THF-d_8 and C_6D_6 (see Fig. S38–S41, ESI†). The ^1H NMR spectra of these reactions suggest the formation of a tetravalent species of the composition "$[Ce\{N(SiHMe_2)_2\}_3]_2(\mu_2\text{-}O_2C_6R_4)$". However, the ceric products appear to be unstable in solution at ambient temperature. In C_6D_6, the formation of $Ce[N(SiHMe_2)_2]_4$ was observed in the reaction with BQ as well as other insoluble products. In THF-d_8, the resulting product seemed more stable but after 24 h in solution also traces of decomposition products were found. The Me_4BQ reaction in C_6D_6 also indicated successful oxidation, however, after 24 h the ^1H NMR spectrum revealed signals for trivalent decomposition products as well as traces of $Ce[N(SiHMe_2)_2]_4$. In THF-d_8, the putatively formed hydroquinolate complex was even less stable, showing signals for trivalent by-products directly after addition of Me_4BQ. In addition, the stability of $\mathbf{4}^{bq}$ was investigated in THF-d_8 showing small amounts of decomposition products like $Ce[N(SiMe_3)_2]_3$ after 24 h (Fig. S42, ESI†).

Regrettably, purification of complexes **8** and **9** was impeded by co-crystallisation with the ceric by-products CeL_4. The crystal structures of **8** and **9** revealed two six-coordinate cerium atoms surrounded by two siloxy ligands, two THF donor molecules and two bridging tetramethyl semiquinolato moieties (Fig. 5). The $Ce1\text{–}O_{silanolato}$ distances are elongated by about 0.1 Å compared to the respective tetravalent compounds **5** and **6** and in

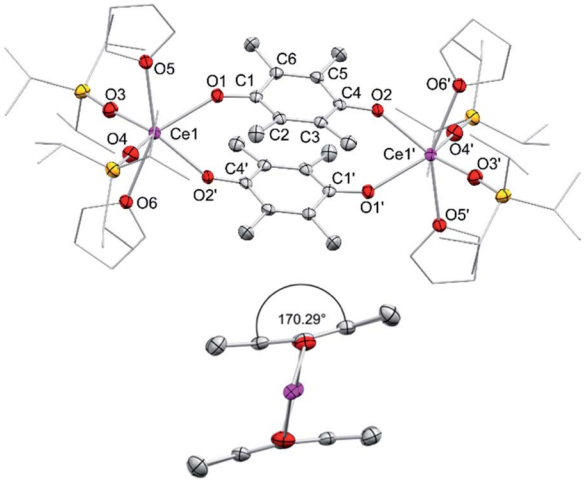

Fig. 5 Top: Crystal structure of $[Ce\{OSi^iPr_3\}_2(thf)_2]_2(\mu_2\text{-}O_2C_6Me_4)_2$ (**9**). Ellipsoids are shown at the 50% probability level. Hydrogen atoms are omitted for clarity. Selected interatomic distances [Å]: Ce1–O1 2.446(7), Ce1–O2 2.422(7), Ce1–O3 2.219(9), Ce1–O4 2.237(6), Ce1–O5 2.648(7), Ce1–O6 2.644 (7), C1–O5 1.306(5), C4–O6 1.307(5), C1–C2 1.458(6), C2–C3 1.401(6), C3–C4 1.449(8), C4–C5 1.463(6), C5–C6 1.388(6), C1–C6 1.463(8). Bottom: side view of $[(Ce\{OSi^iPr_3\}_2(thf)_2)_2(\mu_2\text{-}O_2C_6Me_4)_2]$ (**9**).

accordance with other Ce^{III} siloxides like **3**, $Ce\{OSi(OtBu)_3\}_3(thf)_3$ (2.243(2)–2.249(2) Å), $[Ce\{OSi(OtBu)_3\}_3]_2$ ($Ce\text{–}O_{term}$ 2.186(3)–2.202(3) Å),[26] $Ce\{OSiPh_3\}_3(thf)_3$ ($Ce\text{–}O_{avg}$ 2.222(4) Å)[35] and $[Ce\{OSiPh_3\}_3]_2$ ($Ce\text{–}O_{term}$ 2.141(7)–2.184(6) Å).[27] As expected for semiquinolato ligands the six-membered rings display two shortened C–C and four elongated C–C bonds. Additionally, the six-membered rings are slightly bent in comparison to the flat aromatic hydroquinolato linkers in complexes **4**, **5** and **6** resulting in an angle of 170.34° for **8** and 170.29° for **9**, respectively (see Fig. 5, bottom). Notwithstanding, the bridging radicals engage in significant π-stacking as indicated by close semiquinolato–semiquinolato distances of 3.112 Å for **8** and 3.156 Å for **9**. Overall, complexes **8** and **9** display the same arrangement of the semiquinolato radical bridges as observed in complexes $[LnCl_2(THF)_3(\mu\text{-}Me_4sq)_2]_2$ (Ln = Y, Gd) (Ct···Ct 3.097 Å; Ct = centroid of benzene rings).[13]

To investigate the electronic behaviour of the bridging semiquinolates, X-band EPR spectra of compounds **8** and **9** were recorded from a crystal powder sample at 123 K (Fig. 6). For both complexes cw-EPR spectra are composed of two distinct sets of resonances, one that results from the transition within the Kramers doublet corresponding to $m_j = \pm 1/2$ and one at half-field, $H \approx 160$ mT. The transition for the $m_j = \pm 1/2$ state associates with an axial g tensor with principal components $g_{II} = 2.094$ and $g_{\perp} = 2.032$ for **8** and $g_{II} = 2.088$ and $g_{\perp} = 2.032$ for **9**, respectively. The transition locating at half-field gives rise to a very broad dispersion line with $g_{II} \approx 4.359$ for **8** and $g_{II} \approx 4.351$ for **9**, respectively. Notably, an identical line pattern derives from a frozen 2-Me-THF solution at 77 K; *cf.* Fig. S67, ESI,† for pertinent details. The cw-EPR spectra corroborate the presence of Ce^{3+}, and agree with early work on mononuclear complexes of Ce^{3+}.[36] This indicates a radical–

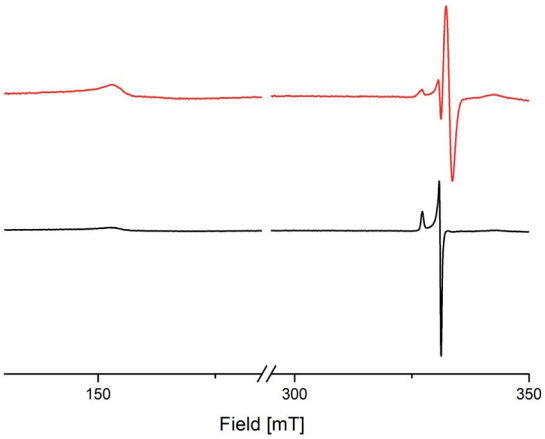

Fig. 6 X-Band cw-EPR spectra of crystalline $[Ce\{OSi(OtBu)_3\}_2(thf)_2(\mu_2\text{-}O_2C_6Me_4)]_2$ (**8**) (black trace) and $[Ce(OSi^iPr_3)_2(thf)_2(\mu_2\text{-}O_2C_6Me_4)]_2$ (**9**) (red trace).

radical π-bonding, as it was recently shown for yttrium and gadolinium semiquinolates $[LnCl_2(thf)_2]_2(\mu_2\text{-}O_2C_6Me_4)_2$ (Ln = Y or Gd).[13] Additionally and also similar to the yttrium semiquinolate, complex **9** shows a signal with a *g* value of 1.999, which most likely results from a non-coupled radical impurity.

Note that the reactions of cerium siloxides **2** and **3** with 1,4-naphthoquinone resulted also in the formation of homoleptic ceric siloxides as well as paramagnetic by-products (*cf.* Fig. S36, ESI†) indicating a similar reactivity as observed for Me_4BQ. Unfortunately, any putative semiquinolate complexes could not be isolated.

Conclusions

Cerium(III) silylamides and siloxides are suitable reagents for assessing the oxidising power/reducibility of differently substituted 1,4-quinones in non-aqueous solutions. The cerium–quinone redox matching is revealed by the ease of formation of Ce^{IV} hydroquinolates $[CeL_3]_2(\mu_2\text{-}O_2C_6R_4)$, in the case of the parent 1,4-benzoquinone (BQ) or when R represents electron-withdrawing groups (Cl, CN). Depending on their reduction potential, alkyl-substituted BQs engage in redox equilibria, with the Ce^{IV} hydroquinolate species being preferentially stable in the solid state, but also afford semiquinolates *via* redox ligand redistribution. The structurally characterized siloxide semiquinolate complexes $[(CeL_2(thf)_2)(\mu_2\text{-}O_2C_6Me_4)]_2$ (L = $OSi(OtBu)_3$, OSi^iPr_3) exhibit a molecular arrangement, recently detected for $[LnCl_2(THF)_3(\mu\text{-}Me_4sq)_2]_2$ (Ln = Y, Gd).[13] The stabilisation of the tetravalent oxidation state in hydroquinolato-bridged complexes $[Ce^{IV}L_3]_2(\mu_2\text{-}O_2C_6R_4)$ was examined by electrochemical measurements, as well as NMR and UV/Vis spectroscopies. In accordance with previous findings,[16,18–20] the stability of the ceric complexes increases in the order of $N(SiMe_3)_2 < OSi(OtBu_3)_3 < OSi^iPr_3$ as supporting ligand, but surprisingly drops in reverse order of the oxidation potential of the 1,4-quinones, being the least stable for the 2,3-dichloro-5,6-dicyano-hydroquinolato congener. The preferred formation of hydroquinolato-bridged silylamides $[Ce\{N(SiMe_3)_2\}_3]_2(\mu_2\text{-}O_2C_6R_4)$ seems kinetically favoured. Finally, the electrochemical reduction of the hydroquinolato-bridged ceric complexes $[Ce^{IV}L_3]_2(\mu_2\text{-}O_2C_6R_4)$ can be mimicked by chemical reduction with cobaltocene, as shown for the isolation and structural characterisation of cerous $[(Ce\{N(SiMe_3)_2\}_3)_2(\mu_2\text{-}O_2C_6H_4)][CoCp_2]_2$. The cerium–quinone redox matching and tuning might be used as a role-model in tetravalent praseodymium and terbium chemistry.

Conflicts of interest

There are no conflicts to declare.

Acknowledgements

We thank the Institute of Organic Chemistry at EKUT for EPR measurements.

Notes and references

1 N. El-Najjar, H. Gali-Muhtasib, R. A. Ketola, P. Vuorela, A. Urtti and H. Vuorela, *Phytochem. Rev.*, 2011, **10**, 353–370.
2 (*a*) N. G. Connelly and W. E. Geiger, *Chem. Rev.*, 1996, **96**, 877–910; (*b*) D. H. Evans, *Chem. Rev.*, 2008, **108**, 2113–2144.
3 (*a*) A. Osyczka, C. C. Moser, F. Daldal and P. L. Dutton, *Nature*, 2004, **427**, 607–612; (*b*) J. F. Allen and W. Martin, *Nature*, 2007, **445**, 610–612; (*c*) J. L. Nevarez, A. Turmo, J. Hu and R. P. Hausinger, *ChemCatChem*, 2020, **12**, 4242–4254.
4 J. M. Campos-Martin, G. Blanco-Brieva and J. L. G. Fierro, *Angew. Chem., Int. Ed.*, 2006, **45**, 6962–6984.
5 M. T. Huynh, C. W. Anson, A. C. Cavell, S. S. Stahl and S. Hammes-Schiffer, *J. Am. Chem. Soc.*, 2016, **138**, 15903–15910.
6 C. Frontana, Á. Vázquez-Mayagoitia, J. Garza, R. Vargas and I. González, *J. Phys. Chem. A*, 2006, **110**, 9411–9419.
7 (*a*) D. Walker and J. D. Hiebert, *Chem. Rev.*, 1967, **67**, 153–195; (*b*) S. B. Bharate, *Synlett*, 2006, **3**, 496–497.
8 (*a*) K. Ohkubo, A. Fujimoto and S. Fukuzumi, *J. Am. Chem. Soc.*, 2013, **135**, 5368–5371; (*b*) N. A. Romero and D. A. Nicewicz, *Chem. Rev.*, 2016, **116**, 10075–10166.
9 (*a*) M. Oh, G. B. Carpenter and D. A. Sweigart, *Acc. Chem. Res.*, 2004, **37**, 1–11; (*b*) S. U. Son, S. B. Kim, J. A. Reingold, G. B. Carpenter and D. A. Sweigart, *J. Am. Chem. Soc.*, 2005, **127**, 12238–12239.
10 (*a*) S. Kitagawa, *Coord. Chem. Rev.*, 2002, **224**, 11–34; (*b*) S. Masaoka, G. Akiyama, S. Horike, S. Kitagawa, T. Ida and K. Endo, *J. Am. Chem. Soc.*, 2003, **125**, 1152–1153.
11 (*a*) B. F. Abrahams, J. Coleiro, B. F. Hoskins and R. Robson, *Chem. Commun.*, 1996, 603–604; (*b*) S. Halis, A. K. Inge, N. Dehning, T. Weyrich, H. Reinsch and N. Stock, *Inorg. Chem.*, 2016, **55**, 7425–7431.
12 J. O. Moilanen, A. Mansikkamäki, M. Lahtinen, F.-S. Guo, E. Kalenius, R. A. Layfield and L. F. Chibotaru, *Dalton Trans.*, 2017, **46**, 13582–13589.

13 T. Han, J. B. Petersen, Z.-H. Li, Y.-Q. Zhai, A. Kostopoulos, F. Ortu, E. J. L. McInnes, R. E. P. Winpenny and Y.-Z. Zheng, *Inorg. Chem.*, 2020, **59**, 7371–7375.

14 (*a*) J. Yuasa, T. Suenobu and S. Fukuzumi, *J. Am. Chem. Soc.*, 2003, **125**, 12090–12091; (*b*) J. Yuasa and S. Fukuzumi, *J. Am. Chem. Soc.*, 2007, **129**, 12912–12913.

15 For examples of other structurally characterised semiquinone complexes, see: (*a*) J.-M. Lü, S. V. Rosokha, I. S. Neretin and J. K. Kochi, *J. Am. Chem. Soc.*, 2006, **128**, 16708–16719; (*b*) H. Nakamori, T. Matsumoto, T. Yatabe, K.-S. Yoon, H. Nakai and S. Ogo, *Chem. Commun.*, 2014, **50**, 13059–13061; (*c*) I.-R. Jeon, B. Negru, R. P. Van Duyne and T. D. Harris, *J. Am. Chem. Soc.*, 2015, **137**, 15699–15702.

16 Â. Domingos, I. Lopes, J. C. Waerenborgh, N. Marques, G. Y. Lin, X. W. Zhang, J. Takats, R. McDonald, A. C. Hillier, A. Sella, M. R. J. Elsegood and V. W. Day, *Inorg. Chem.*, 2007, **46**, 9415–9424.

17 (*a*) F. Sroor and F. Edelmann, in *Cerium: Molecular Structure, Technological Applications and Health Effects*, Nova Science Publishers, Hauppage, N.Y., 2012, pp. 73–106; (*b*) N. A. Piro, J. R. Robinson, P. J. Walsh and E. J. Schelter, *Coord. Chem. Rev.*, 2014, **260**, 21–36; (*c*) Y.-M. So and W.-H. Leung, *Coord. Chem. Rev.*, 2017, **340**, 172–197; (*d*) R. Anwander, M. Dolg and F. T. Edelmann, *Chem. Soc. Rev.*, 2017, **46**, 6697–6709.

18 (*a*) V. Nair, J. Mathew and J. Prabhakaran, *Chem. Soc. Rev.*, 1997, **26**, 127–132; (*b*) V. Nair and A. Deepthi, *Tetrahedron*, 2009, **65**, 10745–10755.

19 Y. Qiao and E. J. Schelter, *Acc. Chem. Res.*, 2018, **51**, 2926–2936.

20 (*a*) O. Eisenstein, P. B. Hitchcock, A. G. Hulkes, M. F. Lappert and L. Maron, *Chem. Commun.*, 2001, 1560–1561; (*b*) M. D. Walter, R. Fandos and R. A. Andersen, *New J. Chem.*, 2006, **30**, 1065; (*c*) P. Dröse, A. R. Crozier, S. Lashkari, J. Gottfriedsen, S. Blaurock, C. G. Hrib, C. Maichle-Mössmer, C. Schädle, R. Anwander and F. T. Edelmann, *J. Am. Chem. Soc.*, 2010, **132**, 14046–14047; (*d*) A. R. Crozier, A. M. Bienfait, C. Maichle-Mössmer, K. W. Törnroos and R. Anwander, *Chem. Commun.*, 2013, **49**, 87–89; (*e*) D. Schneider, T. Spallek, C. Maichle-Mössmer, K. W. Törnroos and R. Anwander, *Chem. Commun.*, 2014, **50**, 14763–14766; (*f*) U. J. Williams, J. R. Robinson, A. J. Lewis, P. J. Carroll, P. J. Walsh and E. J. Schelter, *Inorg. Chem.*, 2014, **53**, 27–29; (*g*) D. Schneider, N. Harmgarth, F. T. Edelmann and R. Anwander, *Chem.–Eur. J.*, 2017, **23**, 12243–12252; (*h*) L. A. Solola, P. J. Carroll and E. J. Schelter, *J. Organomet. Chem.*, 2018, **857**, 5–9; (*i*) N. T. Rice, J. Su, T. P. Gompa, D. R. Russo, J. Telser, L. Palatinus, J. Bacsa, P. Yang, E. R. Batista and H. S. La Pierre, *Inorg. Chem.*, 2019, **58**, 5289–5304.

21 (*a*) M. Gregson, E. Lu, J. McMaster, W. Lewis, A. J. Blake and S. T. Liddle, *Angew. Chem., Int. Ed.*, 2013, **52**, 13016–13019; (*b*) V. Lorenz, B. M. Schmiege, C. G. Hrib, J. W. Ziller, A. Edelmann, S. Blaurock, W. J. Evans and F. T. Edelmann, *J. Am. Chem. Soc.*, 2011, **133**, 1257–1259; (*c*) J. A. Bogart, C. A. Lippincott, P. J. Carroll, C. H. Booth and E. J. Schelter, *Chem.–Eur. J.*, 2015, **21**, 17850–17859; (*d*) R. P. Kelly, L. Maron, R. Scopelliti and M. Mazzanti, *Angew. Chem., Int. Ed.*, 2017, **56**, 15663–15666.

22 (*a*) P. B. Hitchcock, M. F. Lappert and A. V. Protchenko, *Chem. Commun.*, 2006, 3546–3548; (*b*) M. P. Coles, P. B. Hitchcock, A. V. Khvostov, M. F. Lappert, Z. Li and A. V. Protchenko, *Dalton Trans.*, 2010, **39**, 6780–6788.

23 (*a*) I. J. Casely, S. T. Liddle, A. J. Blake, C. Wilson and P. L. Arnold, *Chem. Commun.*, 2007, 5037–5039; (*b*) P. L. Arnold, I. J. Casely, S. Zlatogorsky and C. Wilson, *Helv. Chim. Acta*, 2009, **92**, 2291–2303; (*c*) D. Werner, G. B. Deacon, P. C. Junk and R. Anwander, *Dalton Trans.*, 2017, **46**, 6265–6277; (*d*) U. Bayer, L. Bock, C. Maichle-Mössmer and R. Anwander, *Eur. J. Inorg. Chem.*, 2020, 101–106.

24 (*a*) A. Sen, H. A. Stecher and A. L. Rheingold, *Inorg. Chem.*, 1992, **31**, 473–479; (*b*) J. R. Robinson, C. H. Booth, P. J. Carroll, P. J. Walsh and E. J. Schelter, *Chem.– Eur. J.*, 2013, **19**, 5996–6004; (*c*) D. Werner, G. B. Deacon, P. C. Junk and R. Anwander, *Chem.– Eur. J.*, 2014, **20**, 4426–4438.

25 The reactivity of a series of methyl-substituted 1,4-benzoquinones toward π-allylnickel bromide was probed (yielding ring-allylation in 2- or 6-position), revealing enhanced reactivity of the more easily reduced BQs: L. S. Hegedus and E. L. Waterman, *J. Am. Chem. Soc.*, 1974, **96**, 6789–6791.

26 J. Friedrich, C. Maichle-Mössmer and R. Anwander, *Chem. Commun.*, 2017, **53**, 12044–12047.

27 W. J. Evans, R. E. Golden and J. W. Ziller, *Inorg. Chem.*, 1991, **30**, 4963–4968.

28 H. A. Stecher, A. Sen and A. L. Rheingold, *Inorg. Chem.*, 1989, **28**, 3280–3282.

29 P. S. Gradeff, K. Yunlu, A. Gleizes and J. Galy, *Polyhedron*, 1989, **8**, 1001–1005.

30 U. J. Williams, P. J. Carroll and E. J. Schelter, *Inorg. Chem.*, 2014, **53**, 6338–6345.

31 (*a*) J. Friedrich, Y. Qiao, C. Maichle-Mössmer, E. J. Schelter and R. Anwander, *Dalton Trans.*, 2018, **47**, 10113–10123; (*b*) C. T. Palumbo, I. Zivkovic, R. Scopelliti and M. Mazzanti, *J. Am. Chem. Soc.*, 2019, **141**, 9827–9831; (*c*) A. R. Willauer, C. T. Palumbo, R. Scopelliti, I. Zivkovic, I. Douair, L. Maron and M. Mazzanti, *Angew. Chem., Int. Ed.*, 2020, **59**, 3549–3553.

32 P. G. Eller and R. A. Penneman, *J. Less-Common Met.*, 1987, **127**, 19–33.

33 (*a*) U. Kilimann, R. Herbst-Irmer, D. Stalke and F. T. Edelmann, *Angew. Chem., Int. Ed. Engl.*, 1994, **33**, 1618–1621; (*b*) H. Fang, B. E. Cole, Y. Qiao, J. A. Bogart, T. Cheisson, B. C. Manor, P. J. Carroll and E. J. Schelter, *Angew. Chem., Int. Ed.*, 2017, **56**, 13450–13454.

34 R. D. Shannon, *Acta Crystallogr.*, 1976, **32**, 751–767.

35 P. S. Gradeff, K. Yunlu, T. J. Deming, J. M. Olofson, R. J. Doedens and W. J. Evans, *Inorg. Chem.*, 1990, **29**, 420–424.

36 K. D. Karlin and S. J. Lippard, *Progress in Inorganic Chemistry*, John Wiley and Sons, New York, 1959.